13th IEA Heat Pump Conference
April 26-29, 2021 Jeju, Korea

Modeling of Megawatt R1233zd(E) High Temperature Heat Pump System

JiaTong Jiang[a], Bin Hu[a,*], R.Z. Wang[a], Hua Liu[a,b], Zhiping Zhang[b], Hongbo Li[b]

[a]Institute of Refrigeration and Cryogenics, Shanghai Jiao Tong University, Shanghai 200240, China
[b] SKL of Air-Conditioning Equipment and System Energy Conservation, GREE Electric Appliances, INC. Zhuhai 519070, China

Abstract

With the enactment of the Kigali amendment, the HFCs are falling into disuse and HFOs are proposed to be studied for replacement. R1233zd(E) as a new HTHP working fluid with low GWP has yet to be further developed. The HTHP is an ideal replacement of boiler to supply heat in industry. However, the construction of megawatt unit usually has a huge investment and may not achieve the desired results. Therefore, a mathematical model is imperative to conduct the performance prediction. This paper proposed a model and it can effectively verify the feasibility of the megawatt R1233zd(E) HTHP system, which recovers 60-80℃ waste heat and outputs 100-160℃ pressured water. The conditions of condensation temperature from 90-160℃ with temperature lift of 50K, were calculated and the COP changed in 3.0-3.8. When evaporating at 60℃ and condensing at 110℃, the heat capacity was up to 1.95MW with COP over 3.8. From the results, R1233zd(E) is a reliable refrigerant for both high temperature output and high system efficiency, which will be a direction for future experiments.

Keywords: Dynamic mathematical model; R1233zd(E); High temperature heat pump; Megawatt; COP.

Nomenclature (usually used with subscript)

c	specific heat (J/(kg·K))	α	void fraction
c_p	specific heat (isobaric) (J/(kg·K))	**Subscripts**	
c_v	specific heat (isovolumetric) (J/(kg·K))	*cu*	copper
h	convective heat transfer coefficient (W/(m^2·K))	*C*	condenser
i	specific enthalpy (W/K)	*crit*	critical condition
m	mass flow rate (kg/s)	*COM*	compressor
N	rotation frequency (HZ)	*d*	porous desiccant coating (including pores)
p	pressure (Pa)	*E*	Evaporator
P	electricity consumption (W)	*f*	falling fill area
t	time (s)	*l*	full liquid area
T	temperature (℃)	*r*	refrigerant
u	x component of velocity (m/s)	*TP*	the two-phase refrigerant
v	y component of velocity (m/s)	*rg*	saturated gas of the two-phase refrigerant

* Corresponding author. Tel.: 15021685354; fax: 021-34206548.
E-mail address: hb1223@sjtu.edu.cn.

V	volume (m^3)	rl	saturated liquid of the two-phase refrigerant
λ	conductivity (W/(m·K))	t	tube
ρ	density (kg/m^3)	W	water
l	Characteristic length (m)	TV	throttling valve

1. Introduction

Heat pump is an effective technology for improving grade of thermal energy, especially applied in absorbing heat from air or industrial waste source. In terms of high temperature heat pump (HTHP), it is mainly utilized in industry field to replace boiler [1] (e.g. coal combustion boiler, natural gas boiler, electrical boiler), which can enhance utilization of energy significantly and decrease the consumption of fossil fuels. R245fa has been recognized as the relative appropriate refrigerant for HTHP, which can achieve both high heat sink temperature and COP [2]. In France, there is an R245fa HTHP unit achieves COP of 2.3 at 60℃ heat source and 100℃ output temperature [3], and another large capacity unit (900-1200kW) can reaches 120℃ sink temperature [4]. But with the promulgation of Kigali amendment in the 28th conference of Montreal Protocol, HFCs with high GWP (Global Warming Potential) need to be cut down gradually [5]. To control the emissions of green-house gases, it is necessary and urgent to find better substitutes. HFOs with GWP only 1 has been recommended as potential candidate for both HTHP [6] and Organic Rankine Cycle (ORC) [7]. R1233zd(E), one kind of HFOs, has been studied widely in ORC to replace R245fa with satisfactory result [7, 8]. For HTHP, Kondou and Koyama [9] has achieved huge temperature lift of 80K (70/150℃) with remarkable COP of 5.3, similarly to that of R245fa. There is insufficient study of R1233zd(E) used in HTHP, especially theoretical study. Therefore, it is essential to have careful theoretical research of R1233zd(E) HTHP system for the optimization.

For theoretical research of heat pump, mathematical model is generally the basic key theory. There are some mature methods shown in Fig.1 [10], ranging from simplified lumped parameter model to detailed discretized model. This study mainly bases on the physics modeling methods and not takes black- and grey-box models into account. Lumped parameter model is a common and class physics-based models for heat pump system simulation. Typically, the temperature distribution in the heat exchanger is independent of the coordinates and can be considered as averaged during the heat transformation. This approach effectively simplifies the computation and leads to dimensionality reduction. Yao et al [11] proposed a lumped parameter model for vapor compression system and the prediction models met with experiments within 10% by converting the governing equations of conservation equations to state-space notation. Moving boundary method [12] is generally cooperated with lumped parameter model. Heat exchanger is divided into separate control volumes according single- and two-phase and properties are averaged in each phase. Moving boundary method can reduce computational cost while providing details of phase boundaries, with relative lower accuracy.

The detailed discretized models use finite volume and finite difference to divide the system component into multiple control volumes. From the discretion of governing equations and solving equations simultaneously, the time response of properties can be simulated. Therefore, the discretized models can predict property change over smaller spatial scale. Compared with moving boundary method, finite volume method was fond to be more robust [12]. But as a result of high accuracy, the calculation is more complex and huger [10]. To simplify the formulation, most models neglect the momentum conservation equation. The earliest dynamic research of vapor compression heat pump system can date back to 1985, Gruhle et al [13] proposed an evaporator model (including momentum conservation) and a method for the control of expansion valve. Mac Arthur et al [14] also proposed a discretized model of evaporator but neglecting momentum conservation and verified by experiments. Hermes et al [15] reviewed the modeling methods and simulated the response of a household refrigerator. Bendapudi et al reviewed the dynamic models of vapor compression equipment [16] and proposed a discretized finite volume model (not including momentum conservation) of a vapor compression system and validated with experiments [17]. They also discussed the detailed model formulation and approaches for numerical solution.

For refrigerant, the space for flow is huge inside the shell and the distance between inlet and outlet is relatively short. The pressure drop of refrigerant can be ignored. Therefore, discretized finite volume model (without momentum conservation) is the approach of this study to better simulate the operation of a

megawatt R1233zd(E) HTHP unit.

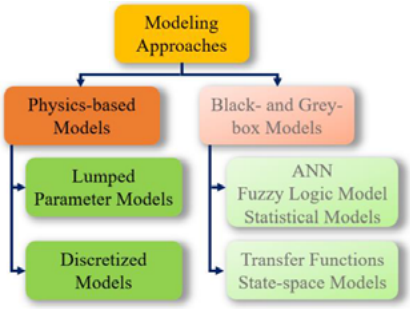

Fig. 1. Classification of modeling approaches for heat pump.

2. Model description

The studied unit is mainly composed of falling film evaporator, double-stage centrifugal compressor, shell-and-tube condenser, electronic expansion valve and flash tank, shown as Fig.2. The double-stage centrifugal compressor is divided into two independent compressors to show the intermediate vapor injection process more clearly.

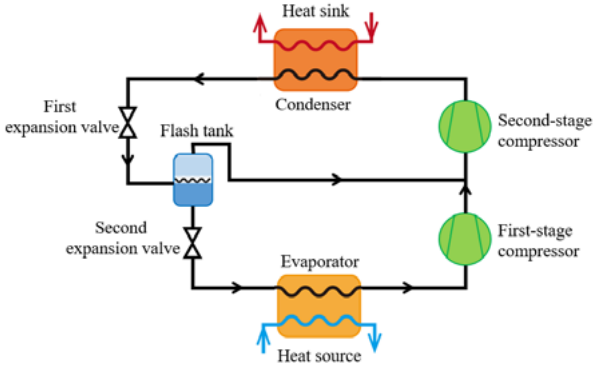

Fig. 2. Schematic of heat pump system cycle

2.1 Compressor model

The type of the compressor is double-stage centrifugal, of which the frequency N_{COM} is 50r/s, the adiabatic efficiency (η_s) is 75%, mechanical efficiency (η_{me}) is 98% and the motor efficiency (η_{mo}) is 97%. Actually, the capacity of centrifugal compressor is controlled by variable inlet guide vanes. In this study, to simplify model the compressor is simulated to operate under wide-open vanes with maximum flow rate. The basic governing equations are shown as equation 1, the mass flow rate $m_{r,COM}$ can be obtained, and given the $i_{r,COMint}$ (enthalpy of refrigerant from evaporator inlet) can get the $i_{r,COMout}$ (enthalpy of condenser outlet). Finally, the power consumption of compressor can be calculated.

$$\begin{cases} m_{r,COM} = N_{COM} V_{COM} \rho_{r,COMin} \\ i_{r,COMout} = \frac{(i_{r,iso-entropy} - i_{r,COMin})}{\eta_s} + i_{r,COMin}, \quad \eta_s = 0.75 \\ P_{COM} = \frac{m_{r,CM}(i_{r,COMout} - i_{r,COMin})}{\eta_{me}\eta_{mo}}, \qquad \eta_{me} = 0.98, \eta_{mo} = 0.97 \end{cases} \tag{1}$$

2.2 Expansion valve

The function of expansion valve is to expand the refrigerant from high pressure and temperature to low pressure and temperature meeting the evaporation condition. At the same time, the expansion can adjust the flow rate of refrigerant by controlling the opening degree of valve to response to the load change. According to equation 2, the mass flow rate $m_{r,TV}$ of the expansion valve is determined by the pressure difference ($p_{r,TVin}$-$p_{r,TVout}$), and the inlet enthalpy $i_{r,TVin}$ is considered to be the same with outlet enthalpy $i_{r,TVout}$ because of the ideal iso-enthalpy throttling process.

$$\begin{cases} m_{r,TV} = K\sqrt{(p_{r,TVin} - p_{r,TVout})\rho_{r,TVin}} \\ i_{r,TVin} = i_{r,TVout} \end{cases} \tag{2}$$

2.3 Evaporator

In this model, the four tube-passes falling film evaporator is applied, with the arrangement of tubes inside the evaporator approximately displayed in Fig. 3 and detailed number of tubes listed in Table 1. The outer and inner diameter of tube (light tube) inside evaporator and condenser are all 19.05mm and 16.2mm respectively. The general flow patterns of a falling film evaporator can be divided into film shape, column shape and dry shape from top to bottom. There will be pluges of heat trasfer coefficent when drop spot occurs, so the heat transfer process needs to be discussed seperatelly. The heat transfer coefficient inside tube of evaporator and condenser is the same, calculated as equation 7. The coefficient of refrigerant outside the evaporator in the falling film area is estimated as equation 8 [18]. When the liquide film evaporates to dry out, the coefficent of heat transfer follows equation 10. In full liquid area, pool boiling heat tansfer coefficient is calculated as the Cooper formula (equation 10) [19].

$$h_W = \frac{\lambda Nu}{Di} = \frac{\lambda_w * 0.023 * Re_w^{0.8} Pr_w^{0.4}}{Di} \tag{7}$$

$$\begin{cases} h_{r,f} = Kh_p \\ K_f = (1 - 0.335\frac{d_t}{d_{t,sta}})[2.059 + 2.37\frac{q_{i,j}}{q_{crit}} + 7.793(\frac{q_{i,j}}{q_{crit}})^2] \end{cases} \tag{8}$$

$$\begin{cases} h_{r,f} = Kh_p \\ K_d = \frac{K_{f,crit}}{Re_{crit}} Re_r, \qquad Re_r = \frac{4m_r}{\mu_r} \\ \frac{Re_r}{Re_{crit}} = (\frac{q_{i,j}}{q_{crit}})^2, \qquad Re_{crit} = 2(0.00339 * q_{crit} + 82.3) \end{cases} \tag{9}$$

$$\begin{cases} h_{r,l} = 55 * q_{i,j}^{0.67} M_r^{-0.5} p_r^m (-lgp_r)^{-0.55} \\ m = 0.12 - 0.21gR_p, \qquad R_p = 0.3 - 0.4\mu m \end{cases} \tag{10}$$

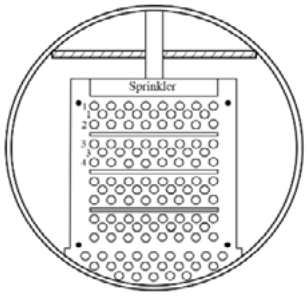

Fig. 3. Inner structure of falling film evaporato

Table 1. Number of tubes of heat exchanger

Tube Row	No. of tubes	
	Evaporator	Condenser
1	19	12
2	19	23
3	19	24
4	10	23
5	19	24
6	19	24
7	19	25
8	10	24
9	19	25
10	19	23
11	9	24
12	10	23
13	24	22
14	21	21
15	18	18
16	15	13
17	10	8
Total	279	356

2.4 Condenser

A horizontal shell-and-tube condenser with one shell process and two tube processes, shown as Fig. 4. The tubes of condenser adopted an equilateral triangle arrangement with total 356 tubes and the number of every row is listed at Table 1. Because of the staggered arrangement, condensate may not fall directly on the tube beneath as Fig. 5 shown, but falls on the slanted and middle tubes, which is defined as lateral drainage. since the condensate drains over intermediate tube, the rows number of tubes should be adopted as Fig.5 reflected. From some ideal simplification, almost half of one tube volume is flooded. Above the analysis, Eissenberg et al [20] proposed the heat transfer coefficient of condensation according different rows (equation 11). From the equation, hn is set to the valve of h1 which is the first row of condensation.

$$\begin{cases} \frac{h_n}{h_1} = 0.7974 + 0.2327n^{-1/5} \\ \frac{h_1}{\lambda_1}[\frac{\mu_l^2}{g\,\rho_l^2}]^{1/3} = 1.523(\frac{4m_1}{\mu_l})^{-1/3} \end{cases} \tag{11}$$

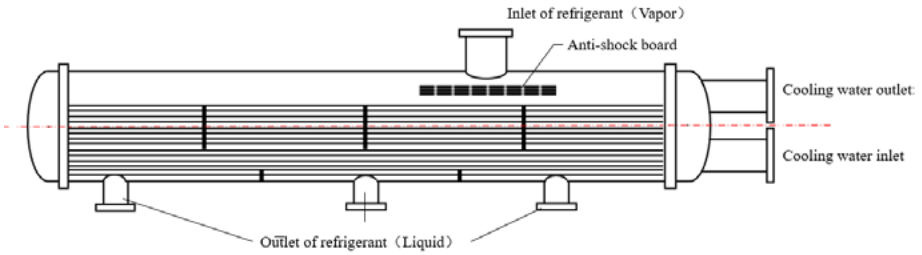

Fig. 4. Structure diagram of horizontal shell-and-tube condenser<1-2>

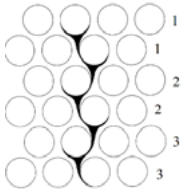

Fig. 5. Pure lateral drains and tube rows.

Here, the methods for control volume division and finite difference of condenser are described carefully, and they are similar to evaporator. With the method of finite volume, heat exchanger is divided into limited control volume according to the inner node method, shown in Fig.6. In condenser, superheated vapor enters

from top and passes through the anti-shock plate, then it flows downward more uniformly. The vapor condenses on the surface of the heat exchange tube, and the condensation liquid gradually flows downward due to gravity. Cooling water flows into heat exchanger from low tubes and out of heat exchanger from up tubes. When cooling water is out of low tubes ($i_{9\text{-}N}j_{M+1}$ side), there is a mixed process of tubes of i_9-i_N which is assumed as well mixed to T_{wmid} and the inlet temperature of i_1-i_8 is also T_{wmid}. The results of discretized equations (3-7) are in appendix, and it should be noted that the boundary of the model like nodes i_0j_1, i_1j_{M+1}, $i_{N+1}j_1$ and $i_{N+1}j_M$, using Taylor expansion method to discretize. Because of the flow direction of refrigerant and water, second-order upwind difference scheme is used as discretization method of governing equations. Second-order center difference is called for discretization of tube wall governing equations due to no fluid flowing and only energy conservation.

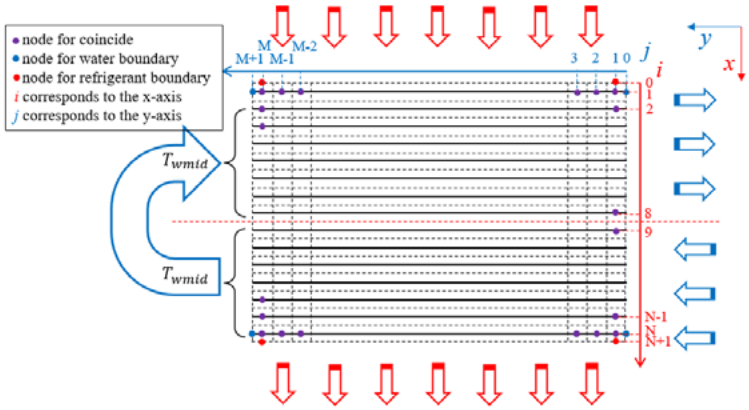

Fig. 6. Schematic of discretized finite volume of condenser.

2.5 *Flash tank model*

The flash tank mainly works to adjust the mass flow rate of vapor injection. The pressure inside flash tank is same with outlet of first expansion valve and first-stage compressor. The saturated vapor is injected to the middle of compressor and mix with the superheated vapor of outlet first-stage compressor to a moderate superheat temperature. At the same time, the mass flow rate of main stream (evaporator) contains constant.

3. Calculation algorithm

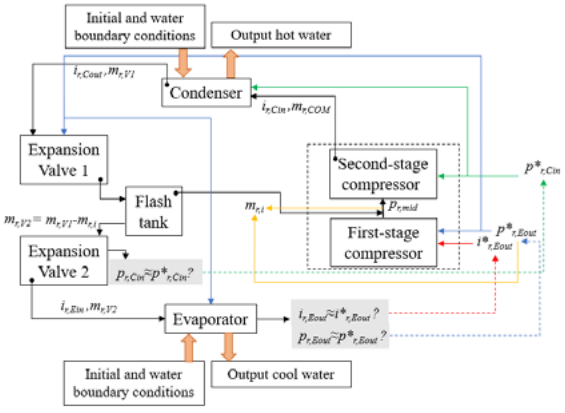

Fig. 7. Framework of the system simulation of the HTHP

The calculation algorithm of double-stage compression with intermediate vapor injection heat pump system is shown in Fig.7. First, the evaporation pressure ($p^*_{r,Eout}$), enthalpy of evaporator outlet ($i^*_{r,Eout}$) and condensation pressure ($p^*_{r,Cin}$) are assumed and the pressure between two-stage compressor is set, then the mass flow rate of intermediate vapor injection can be determined. Refrigerant flows through compressor, condenser and expansion valves, with current pressure of condensation ($p_{r,Cin}$) calculated. With current $p_{r,Cin}$ as initial input $p^*_{r,Cin}$, iterate $p_{r,Cin}$ until $p_{r,Cin}$ is equal to $p^*_{r,Cin}$. Similarly, $i_{r,Eout}$ and $p_{r,Eout}$ can be updated after calculating the properties of evaporator and set $i_{r,Eout}$ and $p_{r,Eout}$ as assumed value of initial input until they are equal. Transient properties of refrigerant, tube and water during the operation can be estimated by the repeated calculation of iteration. The calculation is finished by C++ program.

4. Results and discussion

The simulated system is equipped with intermediate vapor injection system, in which saturated vapor from flash tank was injected to the suction port of Second-stage compressor. Therefore, there will be an optimum mid-pressure injection. Fig. 8-11 shows the system performances varying with the increasing of mid-pressure, and the calculated working condition is evaporating at 55℃, condensing at 80℃, 2℃ subcooling at the outlet of condenser and mass flow rate of First-stage compressor constant at 15kg/s. In Fig.8, the vapor injected mass flow rate shows a downward trend. When the open degree of first-stage throttle remains unchanged, the pressure difference between inlet and outlet of throttle shrinks, and mass flow rate decreases (according equation 2). Further, the superheat of Second-stage compressor discharge decreases slightly, which is mainly due to the physical properties of R1233zd(E) that the slope of isentropic line is larger than saturated gas line and the distance between them is closer in higher temperature area. Therefore, the refrigerant compressed from mid-pressure to Second-stage will get the state closer to saturated gas line when mid-pressure higher. The heating capacity is larger than 2 MW, and decreases with the mid-pressure increasing, which is mainly due to the decreasing of mass flow rate in condenser (shown as Fig. 9). In Fig. 10, the power consumption of First-stage and Second-stage compressor are compared and the consumption of Second-stage compressor decreases with the increasing of mi-pressure. The decline is mainly because of the decrease of injected vapor mass flow rate and enthalpy difference. The increasing enthalpy difference with mi-pressure increasing is the reason of power consumption of First-stage compressor increase. Last, the system COP is calculated, shown in Fig. 11. There is a peak value with the increasing of mid-pressure, therefore, an optimum mid-pressure exists. The COP is calculated according to the definition that ratio of heating capacity to power consumption. Actually, the heating capacity and total power consumption are both decreasing, so, the changing trend of COP is owing to the relative changing trend of them.

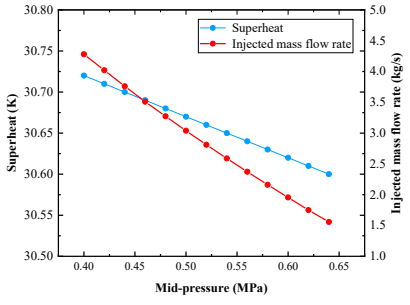

Fig. 8. Variation of superheat of compressor and injected vapour mass flow rate with mid-pressure increasing

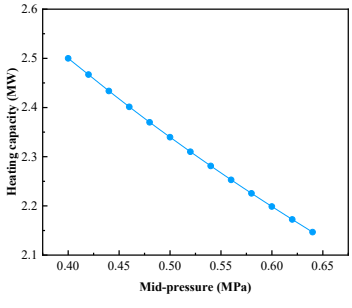

Fig. 9. Variation of heating capacity with mid-pressure increasing

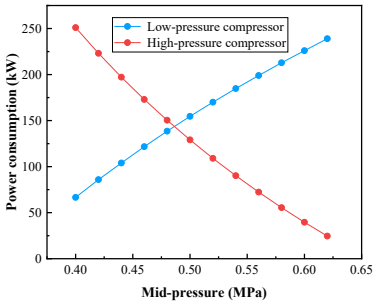

Fig. 10. Variation of power consumptions of First-stage and Second-stage compressor with mid-pressure increasing

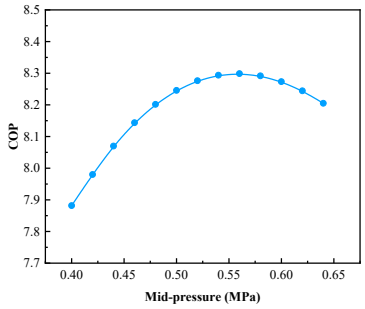

Fig. 11. Variation of COP with mid-pressure increasing

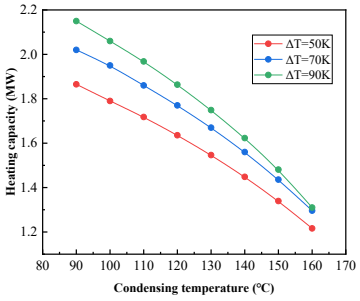

Fig. 12. Variation of heating capacity with condensing temperature increasing (in different ΔT)

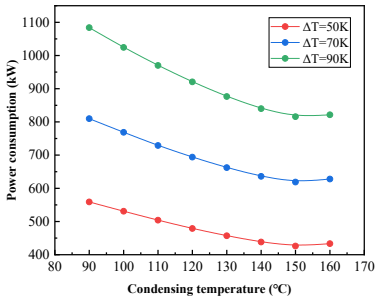

Fig. 13. Variation of power consumption with condensing temperature increasing (in different ΔT)

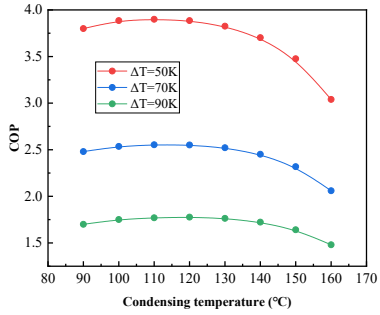

Fig. 14. Variation of COP with condensing temperature increasing (in different ΔT)

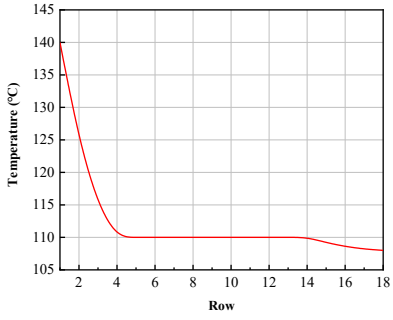

Fig. 15. The temperature distribution of refrigerant inside shell-tube condenser according to the tube row

Further, the system performance in different working conditions are simulated at fixed temperature lift and optimum mid-pressure injection (evaluated as equation12 [21]), shown as Fig12-14. Heating capacity reduces with the condensing temperature increasing (Fig.12), which is mainly attributed to the enthalpy difference decreasing in higher temperature area. At the same time, the heating capacity decreases with the temperature lift dropping, which is owing to that higher evaporation temperature leads to higher optimum mid-pressure and less injected mass flow rate. In Fig. 13, the total power consumption decreases with the absolute slope smaller. The power consumption increases with the temperature lift larger. Even the heating capacity of condition ΔT=90K higher than other, the higher power consumption decides the COP of ΔT=90K is the smallest. And from the comprehensive consideration of heating capacity and power consumption, the COP also has a fluctuating change with the increasing of condensing temperature (shown as Fig. 14). The change is also because of the different reduced rate of heating capacity and power consumption.

$$p_{opt} = \sqrt{p_e p_c} \tag{12}$$

To reveal the inner detailed heat transfer process, temperature distribution of refrigerant inside shell according to the tube row is reflected as Fig. 15. Initially, cooling water (100℃, 115kPa) is pumped to heat

exchange tube of condenser with 32L/s, and the vapor refrigerant (110℃ and 1.28MPa), with about 30℃ superheated. In the first three rows, the superheated refrigerant vapor exchange sensible heat with tube. In the 4-14th row, refrigerant condenses to liquid gradually and exchange latent heat with tube. During the condensation process, the condensate flows from top to full liquid area, therefore, some single-phase heat transfer also appears in two-phase heat transfer area. In the bottom of condenser, there is full liquid area, with saturated liquid cooling to subcooled liquid. The outlet temperature of refrigerant in condenser is about 108℃, with about 2℃ subcooled.

5. Conclusion

In this paper, a mathematical model of megawatt HTHP system adopting R1233zd(E) refrigerant is built. From the discretization of governing equations and the division of limited finite volume, parameters at each control volume can be obtained. The optimum injection mid-pressure is estimated, and due to the physical properties of R1233zd(E), the injected mass flow rate dropping with the increasing of mid-pressure. To predict the operation performance of megawatt R1233zd(E) HTHP, the conditions of condensation temperature from 90-160℃ with temperature lift of 50K, 70K and 90K were calculated. In the condition of 50K temperature lift, he COP changed in 3.0-3.8, and there is a peak value in the range. When evaporated at 60℃ and condensed at 110℃, the heat capacity of this heat pump system was up to 1.9MW with COP above 3.8 during stable operating. From the results of model, R1233zd(E) is kind of a reliable refrigerant for both high temperature output and high system efficiency, which will be a direction for future experiments.

6. Copyright

By submittal of his or her full paper to the Agency for the 13th Heat Pump Conference, the author(s) assumes full responsibility for ensuring that his or her paper does not infringe on another party's intellectual property rights, which include copyright and agree that the paper has not previously been submitted for publication elsewhere. Furthermore, the author, by submittal of his or her conference paper to the conference, grants publishing rights of that paper to the Agency for the 13th Heat Pump Conference, which may:

1. Publish or arrange to publish the paper as part of the Conference proceedings,
2. Copy and distribute the paper in its entirety in print and electronic form, and
3. Copy and distribute excerpts from the paper.

Acknowledgements

This research work was founded by State Key Laboratory of State Key Laboratory of Air-conditioning Equipment and System Energy Conservation (ACSKL2018KT1204) and Fundamental Research Funds for the Central Universities (18X100040029). The authors gratefully acknowledge the financial support from the Research Council of Norway and user partners of HighEFF (Centre for an Energy Efficient and Competitive Industry for the Future, an 8-year Research Centre under the FME-scheme).

References

[1] Zhang J, Zhang H H, He Y L, et al. A comprehensive review on advances and applications of industrial heat pumps based on the practices in China. Applied Energy, 2016, 178:800-825.
[2] Annex 35 IEA. Application of Industrial Heat Pumps, Final report, Part 1. Report No. HPP-AN35e1. 2014.
[3] Lee G, Lee B, Cho J, Ra H-S, Baik Y, Shin HK, et al. Development of steam generation heat pump through refrigerant replacement approach. In: 12th IEA Heat Pump Conference, Rotterdam; 14-17 May, 2017. p. 1-10.
[4] Peureux JL, Sicard F, Bobelin D. French industrial heat pump developments applied to heat recovery. In: 11th IEA Heat Pump Conference, Montreal, Canada; May 12, 2014.
[5] http://conf.montreal-protocol.org/meeting/mop/mop-28/final_report/English/MOP28-Dec1.docx (Ozone Sec Secretariat Conference Portal).
[6] Honeywell. Solstice refrigerants roadmap: The future of refrigerants. Brochure FPR-004-2016-09-EN.

2016. p. 1e2.
[7] Eyerer S, Wieland C, Vandersickel A, et al. Experimental study of an ORC (Organic Rankine Cycle) and analysis of R1233zd-E as a drop-in replacement for R245fa for low temperature heat utilization. Energy, 2016, 103(12):660-671.
[8] Yang J, Ye Z, Yu B, et al. Simultaneous experimental comparison of low-GWP refrigerants as drop-in replacements to R245fa for Organic Rankine cycle application: R1234ze(Z), R1233zd(E), and R1336mzz(E). Energy, 2019, 173:721-731.
[9] Kondou C, Koyama S. Thermodynamic assessment of high-temperature heat pumps using low-GWP HFO refrigerants for heat recovery. Int J Refrig 2015;53:126e41.
[10] Anurag Goyal, Srinivas Garimella. Generalized transient simulation of two-phase heat exchangers using zeotropic fluid mixtures. Int J Refrig 2019:105:120-134.
[11] Yao, Y., Huang, M., Chen, J. State-space model for dynamic behavior of vapor compression liquid chiller. Int. J. Refrig, 2013, 36 (8), 2128–2147.
[12] Bendapudi S, Braun J E, Groll E A . A comparison of moving-boundary and finite-volume formulations for transients in centrifugal chillers. Int. J. Refrig, 2008, 31(8):1437-1452.
[13] Gruhle, W.D., Isermann, R., 1985. Modeling and control of a refrigerant evaporator. J. Dyn. Syst. Measurem. Control 107 (4), 235–240.
[14] MacArthur, J.W., Grald, E.W., 1989. Unsteady compressible two-phase flow model for predicting cyclic heat pump performance and a comparison with experimental data. Int. J. Refrig. 12 (1), 29–41.
[15] Hermes, C.J., Melo, C., 2008. A first-principles simulation model for the start-up and cycling transients of household refrigerators. Int. J. Refriger. 31 (8), 1341–1357.
[16] Bendapudi, S., Braun, J.E., 2002. A Review of Literature on Dynamic Models of Vapor Compression Equipment. ASHRAE, Atlanta, Gap.
[17] Bendapudi, S., Braun, J.E., Groll, E.A., 2005. Dynamic model of a centrifugal chiller system–model development, numerical study, and validation. ASHRAE Trans. 111 (1).
[18] Roques JF, Thome JR. Falling films on arrays of horizontal tubes with R-134a, Part II: flow visualization, onset of dryout, and heat transfer predictions. Heat Transfer Eng 2007;28(5):415–34.
[19] Cooper MG. Saturation nucleate pool boiling - a simple correlation. Int Chem Eng Symp Ser 1984;86:785–92.
[20] Eissenberg, David Martin, Noritake, H.M., 1970. Computer model and correlations for prediction of horizontal-tube condenser performance in sea water distillation plants. Technical report, Oak Ridge National Laboratory.
[21] S. M. Zubair, M. Yaqub and S. H. Khan, 1996. Secondlaw-based thermodynamic analysis of two-stage and mechanical-subcooling refrigeration cycles, Int. J. Refrig. 19:506